



مجلة التربوي
Journal of Educational
ISSN: 2011- 421X
Arcif Q3

معامل التأثير العربي 1.5
العدد 19



مجلة التربوي

مجلة علمية محكمة تصدر عن كلية التربية

جامعة المرقب

العدد التاسع عشر
يوليو 2021م

هيئة تحرير
مجلة التربوي

- المجلة ترحب بما يرد عليها من أبحاث وعلى استعداد لنشرها بعد التحكيم .
 - المجلة تحترم كل الاحترام آراء المحكمين وتعمل بمقتضاها .
 - كافة الآراء والأفكار المنشورة تعبر عن آراء أصحابها ولا تتحمل المجلة تبعاتها .
 - يتحمل الباحث مسؤولية الأمانة العلمية وهو المسؤول عما ينشر له .
 - البحوث المقدمة للنشر لا ترد لأصحابها نشرت أو لم تنشر .
- (حقوق الطبع محفوظة للكلية)



ضوابط النشر:

- يشترط في البحوث العلمية المقدمة للنشر أن يراعى فيها ما يأتي :
- أصول البحث العلمي وقواعده .
 - ألا تكون المادة العلمية قد سبق نشرها أو كانت جزءا من رسالة علمية .
 - يرفق بالبحث تزكية لغوية وفق أنموذج معد .
 - تعدل البحوث المقبولة وتصحح وفق ما يراه المحكمون .
 - التزام الباحث بالضوابط التي وضعتها المجلة من عدد الصفحات ، ونوع الخط ورقمه ، والفترات الزمنية الممنوحة للتعديل ، وما يستجد من ضوابط تضعها المجلة مستقبلا .

تنبيهات :

- للمجلة الحق في تعديل البحث أو طلب تعديله أو رفضه .
- يخضع البحث في النشر لأولويات المجلة وسياساتها .
- البحوث المنشورة تعبر عن وجهة نظر أصحابها ، ولا تعبر عن وجهة نظر المجلة .

Information for authors

- 1- Authors of the articles being accepted are required to respect the regulations and the rules of the scientific research.
- 2- The research articles or manuscripts should be original and have not been published previously. Materials that are currently being considered by another journal or is a part of scientific dissertation are requested not to be submitted.
- 3- The research articles should be approved by a linguistic reviewer.
- 4- All research articles in the journal undergo rigorous peer review based on initial editor screening.
- 5- All authors are requested to follow the regulations of publication in the template paper prepared by the editorial board of the journal.

Attention

- 1- The editor reserves the right to make any necessary changes in the papers, or request the author to do so, or reject the paper submitted.
- 2- The research articles undergo to the policy of the editorial board regarding the priority of publication.
- 3- The published articles represent only the authors' viewpoints.





Influence of annealing and Hydrogen content on structural and optoelectronic properties of Nano-multilayers of a-Si:H/a-Ge: H used in Solar Cells

Ibrahim A. Saleh¹, Tarek M. Fayeze^{*2}, Mustafah M. A. Ahmad²
¹Physics Department, Faculty of Science, Benghazi University, Libya
²School of physics, Sebha University, Libya
^{*}tar.ahmad@sebhau.edu.ly

Abstract

Nano-multilayers (NMLs) of a-Si:H/a-Ge: H were prepared at 200°C by alternating deposition from SiH₄ and GeH₄ plasmas in a computer-controlled four chamber glow-discharge deposition system with capacitive coupled diode reactors. IR spectroscopy and scanning electron microscope (SEM) were used to study the structural changes after annealing at 300 and 450°C for 8 h. The annealed multilayers exhibit surface and bulk degradation with formation of bumps and craters. The electrical measurements results reveal that the increase of electrical conductivity, while optical energy gap is decreased with increasing the annealing temperature and/or time is partially due to formation of H bubbles in the Ge layers and partially due to crystallization effects. On the other hand it was found that the activation energy of crystallization deduced from the annealing time dependence of the conductivity using Avrami's equation is structural dependent.

Keywords Nano-multilayers (NMLs), a-Si:H/a-Ge: H, structure, electrical conductivity, crystallization, Avrami's equation

I. Introduction

Amorphous silicon based semiconductors Nano-multilayers (NMLs) of a great interest for device applications. Nano-multilayers of a-Si:H/a-Ge:H are used as a new type of narrow bandgap materials for amorphous silicon-based solar cells [1]. High efficiency solar cells are necessary to convert solar energy to electrical energy at low cost [2]. Since the quality of a-Si_{1-x}Ge_x:H is not as good as that of a-Si:H, some attempts were carried out to improve the optical and electrical properties of a-Si_{1-x}Ge_x:H by producing it from ultrathin layers of a-Si:H/a-Ge:H [3-9]. In this paper, the effect of hydrogen dilution and hydrogen bond configuration on the quality of Nano-multilayers of a-Si:H/a-Ge:H were investigated.

II. Experimental

The Nano-multilayers(NMLs) of a-Si:H/a-Ge:H were prepared by alternating deposition from SiH₄ and GeH₄ plasmas in a computer-controlled four chamber glow-discharge deposition system with capacitively coupled diode reactors. At a substrate temperature of



200°C, a RF of 13.6 MHz, aRF power of 10 W, a pressure of about 0.18 mbar and a gas flow of 5 sccm in the SiH₄ chamber and 0.32 mbar and a gas flow of 0.25-2 sccm of H₂-GeH₄ in the GeH₄, (NMLs) of a-Si:H/a-Ge:H films were grown on quartz substrates for optoelectronic characterization and on crystalline Si for composition analysis. The (NMLs) of a-Si:H/a-Ge:H structures with well layer thickness of 1.6–8 nm and a barrier layer thickness of 3nm and the other set with barrier layer thickness of 1.6–9 nm and well layer thickness of 1.2 and 2 nm were prepared for the measurements. The individual thickness of a-Si:H barrier layer d_{Si} was varied by changing the deposition time, while the well layer thickness d_{Ge} of a-Ge:H was controlled by changing the hydrogen dilution ratio $[H_2]/[GeH_4]$ as well as by changing the deposition time. The growth rate was kept near 0.1 nm/s for a-Si:H and ranged from 0.1 to 0.4 nm/s for a-Ge:H layers. The total film thickness measured by the Dectak surface profiler was in the range of 300 to 550 nm and the total number of periods was controlled between 60 and 100. The X-ray diffraction (XRD) of the prepared samples has shown that the interface between a a-Ge:H well layer and a a-Si:H barrier layer is atomically abrupt. The period thickness measured by XRD was in good agreement with the period calculated from the total film thickness measured with a Dectak surface profiler and the growth rates of the individual layers in the bulk. Infrared absorption spectra were measured in the range between 400 and 2200 cm^{-1} using a Nicolet Fourier transform infrared spectrometer (model 740). After base line correction, the IR absorption peaks were fitted by Gaussian to obtain the integrated absorption intensity I^* . As the film thickness was usually below 1 μm , the correction proposed by Langford et al. was employed to obtain the integrated absorption I . The optical bandgap E_g was deduced from transmission and reflection measurements using JASCO V-570 UV - vis Spectrophotometer–Instructions. The samples were characterized by the scanning electron microscopy (SEM) after annealing at 300°C for 8 h. For electrical measurements, a co-planer method was used for the dark and photo-conductivity in vacuum. The light source of a tungsten lamp of intensity 100mW/cm² was employed.

III. Results and discussion

3.1. Infrared absorption spectra

Typical infrared (IR) absorption spectra for a-Si:H(3 nm)/a-Ge:H multilayers of thickness $d_{Ge}=1.2$ nm (HD = 20) and $d_{Ge}= 2$ nm (HD =10) are shown in figure (1). For the a-Si:H/a-Ge:H multilayers, major absorption peaks between 500 and 800 cm^{-1} are attributed to Si-H and Ge-H wagging modes and between 1800 and 2200 cm^{-1} due to Si-H and Ge-H stretching modes. The absorption peak near 1880 cm^{-1} is attributed to the stretching vibration of Ge-H groups incorporated into bulk material, while the absorption near 2100 cm^{-1} is associated with the vibration of Si-H and/or Si-H₂ groups located at internal surfaces of voids. The absorption peak near 2000 cm^{-1} was attributed to Ge-H or Ge-H₂ groups at void surface and Si-H groups in compact material [3,10,11].

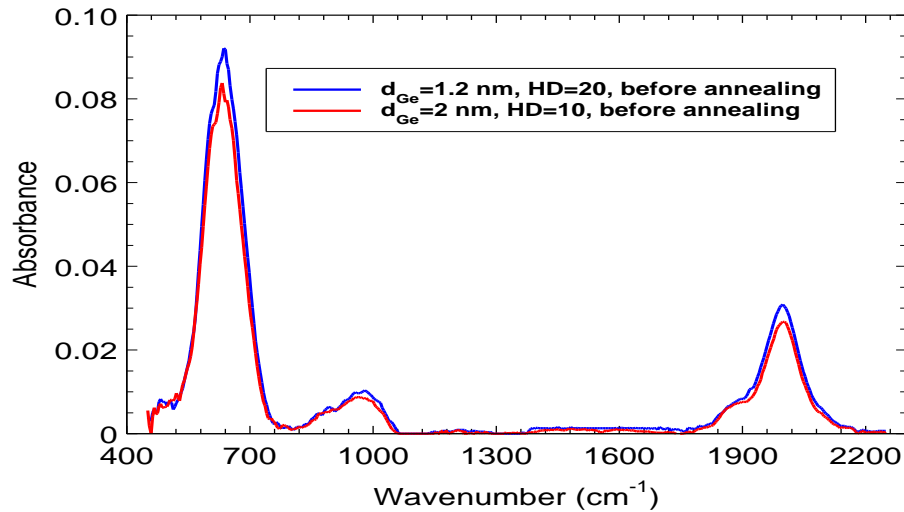


Figure (1): The IR- spectra of untreated a-Si:H(3 nm)/a-Ge:H multilayers of $d_{Ge}=1.2$ and 2 nm.

It seen that the absorbance of the wagging, bending and stretching modes decreases by increasing the well width due to reduction in the total hydrogen content N_H arising from decreasing of the hydrogen dilution during deposition which leads to a decrease of the hydrogen content [12].

The hydrogen evolution from the multilayers of a-Si:H/aGe:H during annealing plays an important role for changes of structure and properties. It is seen that after annealing for 8 h at 300°C and 450°C, the integrated intensity of the waging, bending and stretching bond decreases for the two samples. In the stretching mode range of the wave number, the spectra show that the integrated absorption intensity of Ge-H and Si-H stretching bonds is decreasing after annealing at 300°C and 450°C, indicating that hydrogen moves around in Ge and Si layers and is partially evolved, thus causing a change in the atomic density of the Ge and Si network and also a change in the ratio of $d_{Ge}/(d_{Si}+ d_{Ge})$ which is correlated with the form factor. The hydrogen evolved from Ge and Si layers leads to structural relaxation caused by the annealing preferentially takes place [8,13].

The hydrogen content (N_H) calculated by fitting the stretching mode of a-Si:H(3 nm)/a-Ge:H multilayers of $d_{Ge}=1.2$ nm and $d_{Ge}= 2$ nm before and after annealing (See figures (2) and (3)) is given in table (1). The fitting was done by using Gaussian distribution for calculating the hydrogen content. For brevity see figure (4) for untreated a-Si:H(3nm)/a-Ge:H multilayers of thickness $d_{Ge}=1.2$ nm (HD =20).

It is seen that the total hydrogen content (N_H) is decreasing after annealing at 300 and 450°C due to the evolution of hydrogen from the network during the annealing process.

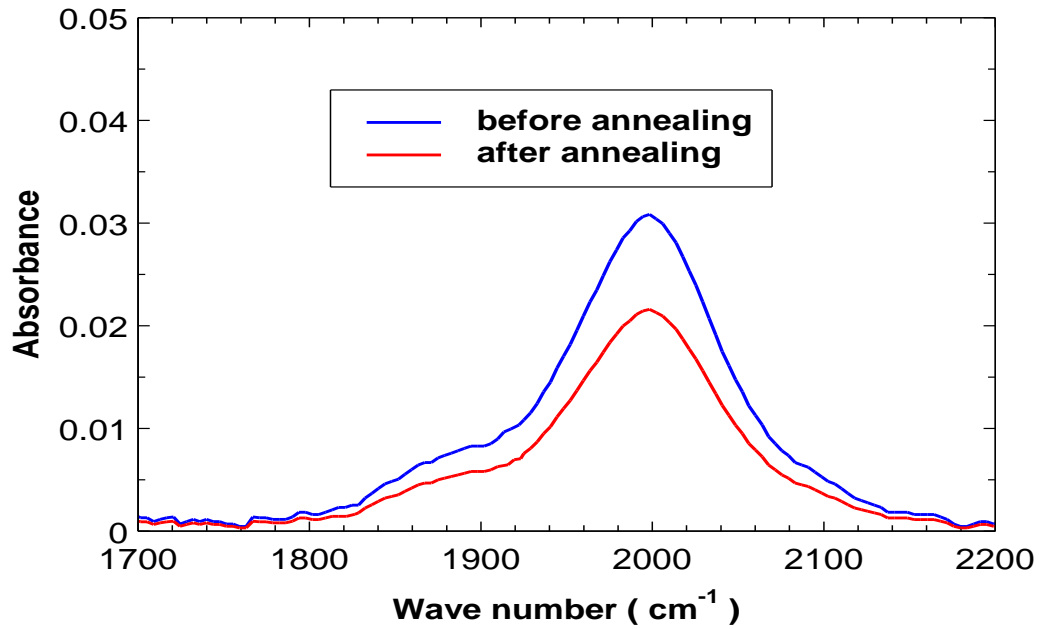


Figure (2): IR- spectra of the stretching mode of a-Si:H (3 nm)/a-Ge:H multilayers of $d_{Ge}=1.2$ nm before and after annealing at 300°C for 8 h.

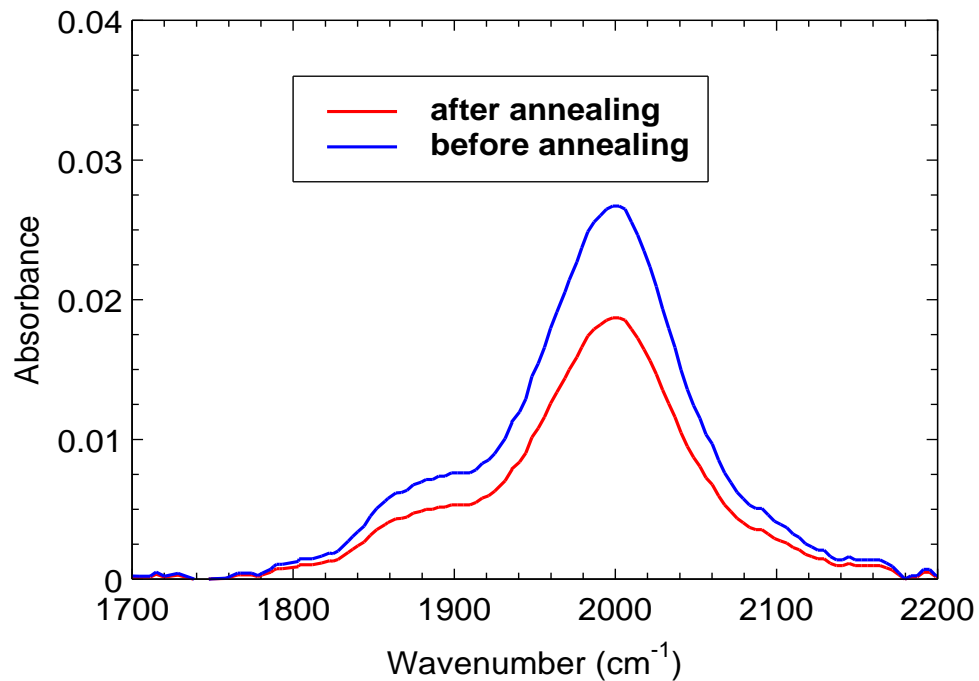


Figure (3): IR- spectra of the stretching mode for a-Si:H (3 nm)/a-Ge:H multilayers of $d_{Ge}=2$ nm before and after annealing at 450°C for 8 h.

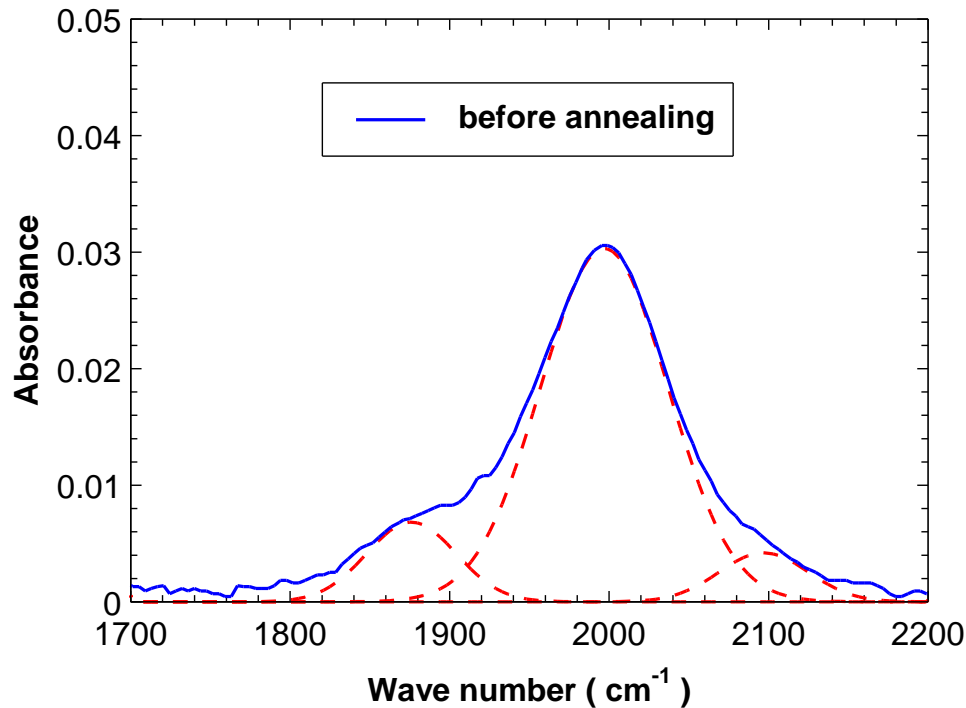


Figure (4): Fitting of IR- spectra in the stretching mode range for a-Si:H (3 nm)/a-Ge:H multilayers of $d_{Ge}=1.2$ nm before annealing.

Table (1): The hydrogen content for the two samples before and after annealing.

Samples	d_{Ge} (nm)	HD	annealing temperature ($^{\circ}C$)	Hydrogen content before annealing (N_H) cm^{-3}	Hydrogen content after annealing (N_H) cm^{-3}
a-Si:H(3 nm)/a-Ge:H	1.2	20	300	2.85×10^{21}	2.03×10^{21}
a-Si:H(3nm)/a-Ge:H	2	10	450	2.64×10^{21}	1.84×10^{21}

3.2 Scanning Electron Microscopy (SEM)

Multilayers of a-Si:H (3 nm)/a-Ge:H were investigated by the scanning electron microscopy (SEM) after annealing at 300 and 450 $^{\circ}C$ for 8 h. Figures (5) and (6) show the SEM images of a-Si:H (3 nm)/a-Ge:H multilayers of $d_{Ge}= 1.2$ and 2 nm and annealed at 300 $^{\circ}C$ and 450 $^{\circ}C$ for 8 h, respectively. It is seen from the images that bumps appear on the surface of the films annealed at 300 $^{\circ}C$ for 8 h{see figure (5)} while craters are



formed on the surface of films annealed at 450°C as shown in figure (6). The hydrogen forming the bubbles arises from the rupture of the Si-H and Ge-H bonds activated by the thermal energy of the annealing temperature [15] and by the energy released from the recombination of thermally generated electron hole pairs. It has been reported that if the initial H content is very high and /or the annealing conditions are very severe creation of craters occurs [16,18]. Thus, craters appeared on the surface of films annealed at 450°C as shown in figure (6).

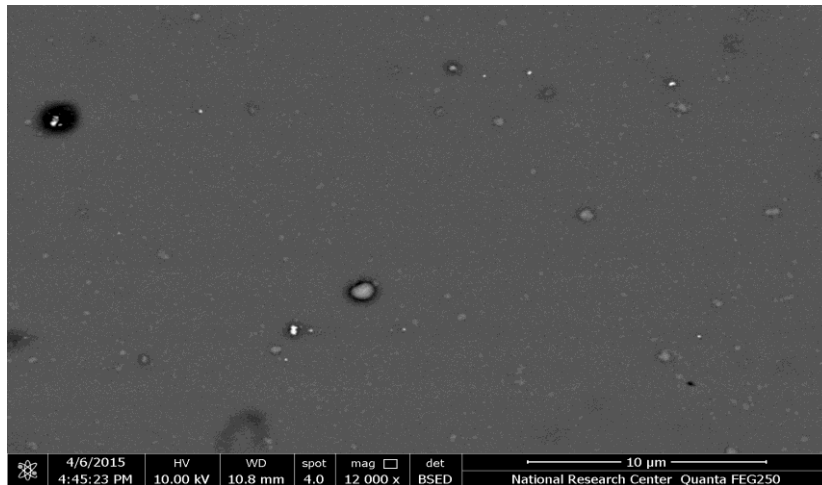


Figure (5): The SEM image for a-Si:H(3nm)/a-Ge:H multilayers of thickness of $d_{Ge}= 1.2$ nm and annealed at 300°C for 8 h.

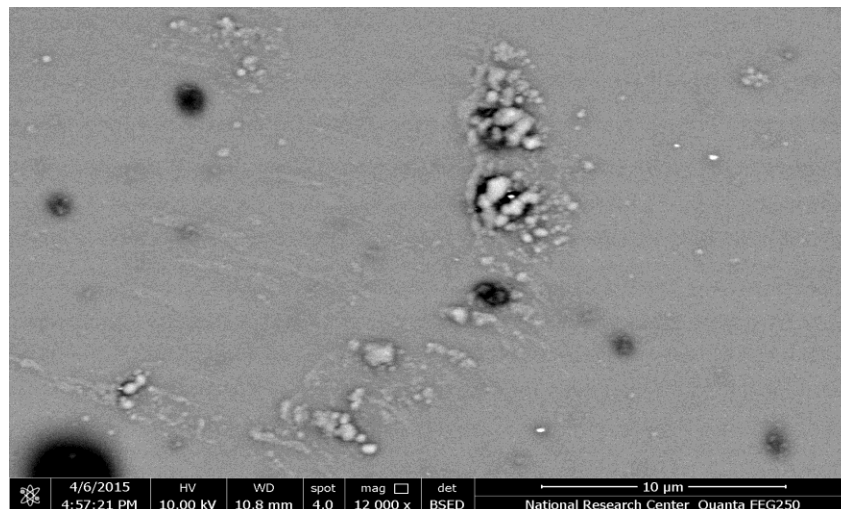


Figure (6): The SEM image for a-Si:H(3nm)/a-Ge:H multilayers of $d_{Ge}=2$ nm and annealed at 450°C for 8h.



3.3. Optoelectronic data

The optical bandgap is useful material parameter that allows comparison of a-Si:H(3 nm)/a-Ge:H multilayers thin films based materials regarding their light absorption properties. Figures (7) and (8) shows the relation between $(\alpha h\nu)^{1/2}$ and $h\nu$ of a-Si:H(3 nm)/a-Ge:H multilayers of thickness $d_{Ge}=1.2$ and 2 nm, respectively. According to Tauc's relation, the optical energy gaps deduced from the plots are given in tables (2) for the two samples before and after annealing.

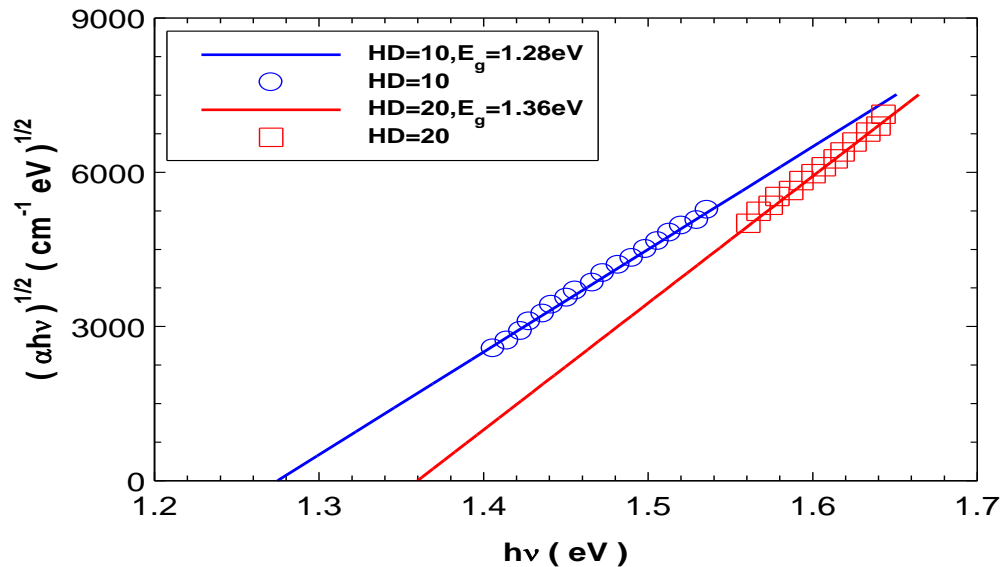


Figure (7): $(\alpha h\nu)^{1/2}$ vs. $h\nu$ for untreated a-Si:H(3nm)/a-Ge:H multilayers of $d_{Ge}=1.2$ nm (HD=20) and $d_{Ge}=2$ nm (HD=10).

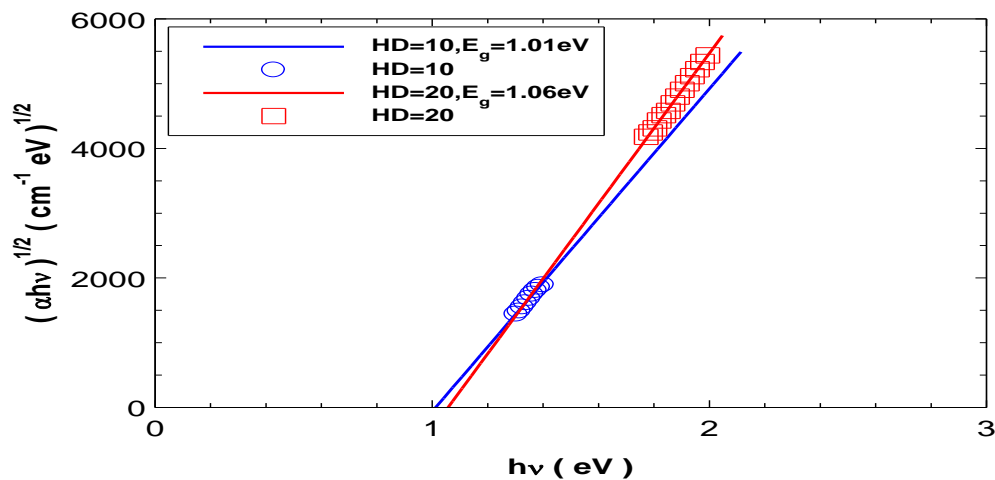


Figure (8) : $(\alpha h\nu)^{1/2}$ vs. $h\nu$ for a-Si:H(3 nm)/a-Ge:H multilayers of $d_{Ge} = 1.2$ nm (HD = 20) and $d_{Ge} = 2$ nm (HD = 10) after annealing.



It seen from table (2) that the optical gap for a-Si:H(3nm)/a-Ge:H multilayers decreases after annealing while the Urbach energy increase. This clearly confirms the very close relationship existing between these two parameters because of the presence of a more or less important density of dangling bonds in the material [9,11,17].

Table (2): The optical energy gap E_g and Urbach energy E_u for a-Si:H(3 nm)/a-Ge:H multilayers.

Sample	d_{Ge} (nm)	before annealing			After annealing		
		N_H (cm^{-3})	E_g (eV)	E_u (meV)	N_H (cm^{-3})	E_g (eV)	E_u (meV)
a-Si:H(3 nm)/a-Ge:H	1.2	2.85×10^{21}	1.36	72	2.03×10^{21}	1.06	79
a-Si:H(3 nm)/a-Ge:H	2	2.64×10^{21}	1.28	96	1.84×10^{21}	1.01	102

The dark and photo- conductivities as a function of temperature for a-Si:H(3 nm)/a-Ge:H multilayers of thickness $d_{Ge}=1.2$ and 2 nm in the temperature range 303- 423 K are shown in figures (9) and (10), respectively. It is seen that the relation between the electrical conductivity and the temperature obey the Arrhenius type equation:

$$\sigma = \sigma_0 \exp(-E_a/k_B T) \quad (1)$$

where σ is electrical conductivity, E_a is the activation energy and k_B is the Boltzmann's constant. The hydrogen content plays an important role for determining electrical conductivity of a-Si:H/a-Ge:H multilayers. The electrical conductivity measured at 300 K and the activation energy calculated from the slopes of the lines for the samples are given in table (3). It is seen that the electrical conductivity increase while activation energy decrease with increasing d_{Ge} due to a decrease in the total hydrogen content as conformed by the previous works [11,14] Also the photo conductivity increases while the photosensitivity decreases with increasing the well width thickness.

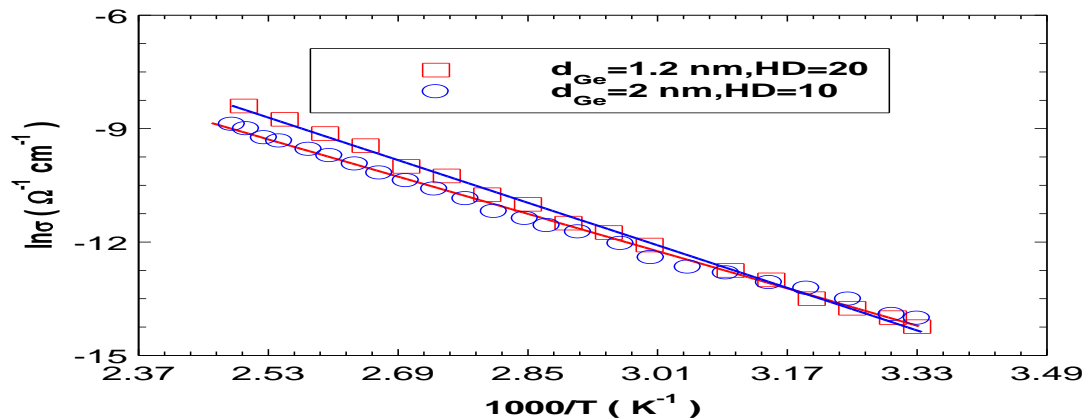


Figure (9): Dark conductivity vs. inverse of temperature for a-Si:H(3 nm)/a-Ge:H multilayers of $d_{Ge} = 1.2$ nm (HD = 20) and $d_{Ge} = 2$ nm (HD = 10).

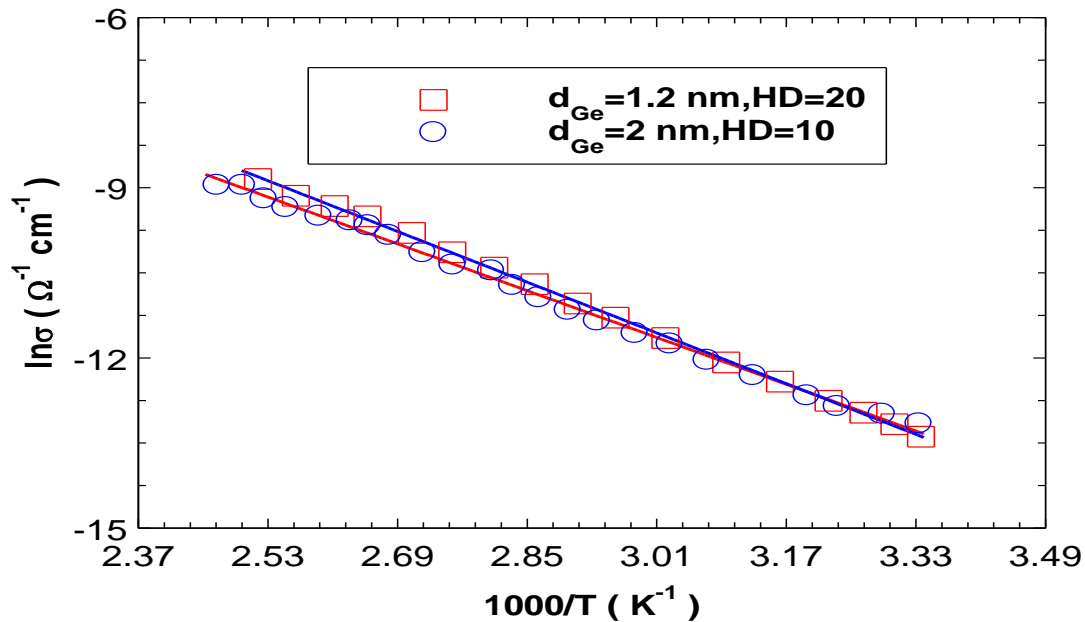


Figure (10): Photo- conductivity vs. inverse of temperature for a-Si:H(3 nm)/a-Ge:H multilayers of $d_{Ge} = 1.2$ nm (HD = 20) and $d_{Ge} = 2$ nm (HD = 10).

Table (3): Dark and photo- conductivity measured at 303 K and the activation energy for untreated a-Si:H(3 nm)/a-Ge:H.

The sample	d_{Ge} (nm)	HD	σ_d ($\Omega^{-1} \cdot \text{cm}^{-1}$)	σ_{Ph} ($\Omega^{-1} \cdot \text{cm}^{-1}$)	σ_{Ph}/σ_d	$E_{a,d}$ (e.V)	$E_{a,Ph}$ (e.V)
a-Si:H(3 nm)/a-Ge:H	1.2	20	5.86×10^{-7}	1.53×10^{-6}	2.61	0.61	0.48
a-Si:H(3 nm)/a-Ge:H	2	10	6.67×10^{-7}	1.64×10^{-6}	2.46	0.53	0.45

The electrical conductivity of a-Si:H(3nm)/a-Ge:H multilayers of $d_{Ge} = 2$ nm as a function of annealing times recorded at different temperatures 493, 523, 553 and 573 K is given figure (11). All samples show the same general behavior where the electrical conductivity increases with increasing the annealing time at constant annealing temperature and becomes constant at high annealing time. This behavior is attributed partially to crystallization occurring in the multilayers and partially to the release of hydrogen from the network depending on the annealing temperature and annealing time. It is known that the conductivity of crystalline material is higher than that of amorphous one since the ordered systems exhibit lower activation energy than the amorphous one. Thus the electrical conductivity measurements as a function of annealing time at constant temperature are used to study the isothermal crystallization kinetics using Johnson-Mehl-Avermi`s (JMA) equation [20].

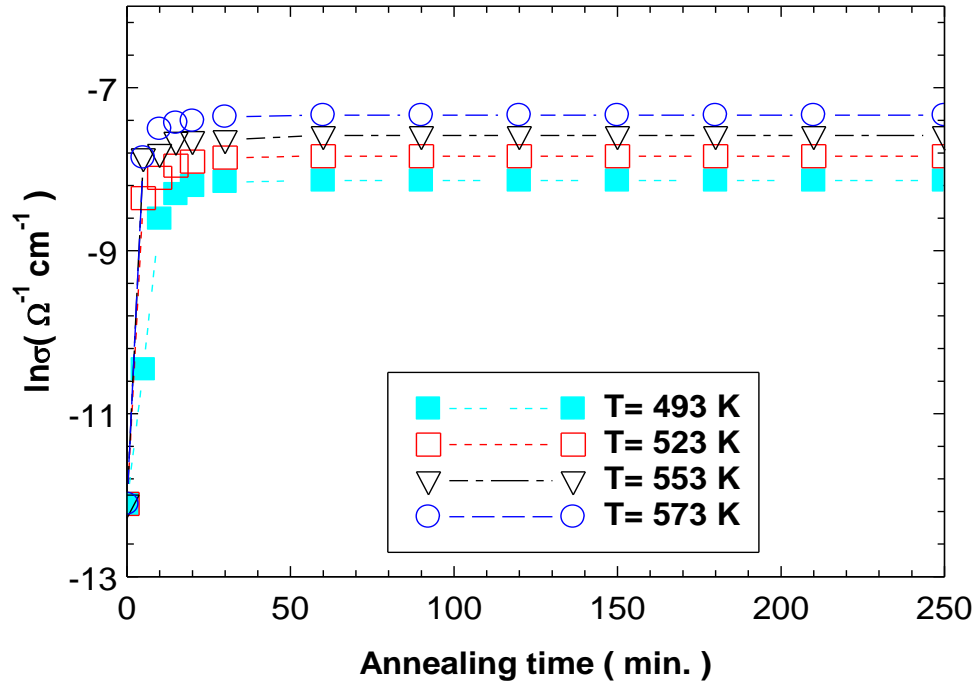


Figure (11): logarithm of the electrical conductivity versus the annealing time at constant annealing temperatures for a-Si:H(3nm)/a-Ge:H multilayers of $d_{Ge}=2$ nm.

It is known that the electrical conductivity of the ordered system is higher than that of amorphous one and the ordered systems exhibit lower activation energy than the amorphous one [19]. Thus the electrical conductivity measurements as a function of annealing time at constant temperature are used to study the othermal crystallization kinetics using Johnson-Mehl-Avermi`s (JMA) equation [20]. in the form:

$$\chi = 1 - \exp[-(kt)^n] \quad (2)$$

Where χ is the volume fraction of the crystalline phases transformed from the amorphous state at time t , n refers to the order of reaction and k is the effective overall reaction rate, which actually reflects the rate of crystallization [20], and it is given by:

$$k = k_0 \exp [-E_c/RT] \quad (3)$$

Here k_0 indicates the number of attempts to overcome the energy barrier. From the results of the conductivity as a function of annealing time the volume fraction χ is calculated from the relation:

$$\chi = (\sigma_t - \sigma_0)/(\sigma - \sigma_0) \quad (4)$$

where σ_0 is the electrical conductivity at zero time, σ_t the electrical conductivity at any time t and σ is the electrical conductivity at the end of saturation (full crystallization). According to JMA equation the value of n can be obtained from the slopes of the plots of $\ln[-\ln(1 - \chi)]$ vs. $\ln(t)$

According to JMA equation the values of (n) are given in table (4) for the studied films measured at 493, 523, 553 and 573 K. Since the volume fraction of the crystallized phases is assumed to depend on the conductivity of the material at any annealing time, we



found that the value of (n) does not depend on the annealing temperature. The values of (k) are given in table (4) for the films. According to equation (3) the values of the activation energies E_c of crystallization for the a-Si:H(3nm)/a-Ge:H multilayers of $d_{Ge}=2$ nm are also given in table (4).

Table (4): Values of n, k and E_c for a-Si:H(3nm)/a-Ge:H multilayers of thickness $d_{Ge}= 2$ nm.

T	n				k				E_c kJ/mol
	493 (K)	523 (K)	553 (K)	573 (K)	493 (K)	523 (K)	553 (K)	573 (K)	
$d_{Ge}=$ 2nm	1.17	0. 757	0. 755	0. 771	7.07×10^{-4}	3.05×10^{-2}	5.16×10^{-1}	7.8×10^{-1}	213.7

For a-Si:H (3nm)/a-Ge:H multilayers of $d_{Ge}=1.2$ nm measured at 573, 623, 673 and 723 K as a function of time, the values of n and values of (k) are given in table (5) for film. According to equation (3) the values of the activation energies E_c of crystallization are given in table (5). The results obtained show that crystallization takes place in Si and Ge layers individually since the crystallization temperature of Ge is around 573 K while that of Si is near 773 K Thus the activation energy of Si layers is higher than that of Ge layers as seen in table (5).

Table(5): Values of n, k and E_c for a-Si:H(3nm)/a-Ge:H multilayers of thickness $d_{Ge}=1.2$ nm.

T	n				k				E_c kJ/mol
	573 (K)	623 (K)	673 (K)	723 (K)	573 (K)	623 (K)	673 (K)	723 (K)	
Ge- Layer	1.15	0.669	0.664	0.761	1.22×10^{-1}	5.13×10^{-1}	6.68×10^{-1}	7.70×10^{-1}	40.41
Si- Layer	0.457	0.325	0.154	0.198	2.70×10^{-3}	1.04×10^{-2}	3.74×10^{-2}	5.77×10^{-2}	72.83

IV. Conclusion

All samples show the same general behavior where the electrical conductivity increases with increasing the annealing time at constant annealing temperature and becomes constant at high annealing time. This behavior is attributed partially to crystallization occurring in the multilayers and partially to the release of hydrogen from the network depending on the annealing temperature and annealing time. The hydrogen content plays an important role for determining the electrical conductivity and optical gap of nano-multilayers a-Si:H/a-Ge:H thin films. The reason in changing optical gap, this may be due to shifting the Fermi level, where increasing shifting the Fermi level above, with bumps large.



Acknowledgements

We would like to thank Professor Mohamed El-Zaidia, Physics Department, Faculty of Science, Menoufia University, Egypt, for his scientific comments and immensely help in achieving our experiments. I am indebted to Prof. Dr. Magdy Said Abo Ghazala, head of Physics Department, Faculty of Science, Menoufia University, Egypt, who supported this work. This work is sponsored by the Libyan ministry of higher education and Benghazi University.

References

- [1] X. Sun, T. Zhang, L. Yu, L. Xu, J. Wang, Scientific Reports 9, 19752 (2019).
- [2] F. T. Si, O. Isabella, M. Zeman, Solar Energy Materials and Solar Cells 163, 9-14 (2017).
- [3] M. S. Abo Ghazala, Physica B 293, 132 (2000).
- [4] P. Haldar, J. L. Harvey, Mater. Scie. Appi. vol. 3, pp. 67 (2012).
- [5] Philips, J. I. Dijkhuis, Phys. Rev. vol. 873, pp. 155202 (2006).
- [6] W.C. Sinke, W.F. van der Weg, S. Roorda, P.C. Zalm, Phys. Rev. B 53, 4415(1996).
- [7] M. Daouahi, K. Zellama, H. Bouchriha, P. Elkaim, Eur Phys J AP10,185 (2000).
- [8] Y. Bouizem, A. Belfedal, J.D. Sib, A. Kebab, L. Chahed, J Phys Condens Matter, 19,356215 (2007).
- [9] A. A. Langford, M. L. Fleet, B. P. Nelson, W. A. Lanford, and N. Maley, Phys. Rev. B 45, 13367 (1992).
- [10] K. W. Jobson and J.P.R. Wells, R.E. I. Schropp, N.Q. Vinh, J.I. Dijkhuis, J. Appl. Phys. 103, 13106 (2008).
- [11] K. Chen, S. Huang, J. Xu, X. Huang, H. Fritzsche, A. Matsuda, G. Gangul, Journal of optoelectronics and Advanced Materials, Vol.4,561(2002).
- [12] M. S. Abo-Ghazala, Phys. Status Solidi C 8, 3099–3102 (2011).
- [13] S. Kannan, **Master of Science**, Department of Physics, The University of Utah (2005).
- [14] R.J. Soukup, N. J. Ianno, S. A. Darveau, C. L. Exstrom, Sol. Energy Mater. Sol. Cells 87,87 (2005).
- [15] W. Beyer and V. Zastrow, J. Non-Cryst. Solids 227-230, 880 (1998).
- [16] W. Paul, D. K. Paul, B. Von Roe Dern, J. Blake, S. Oguz, Phys. Rev. Lett.46, 1016 (1981).
- [17] J. Tauc, in Amorphous and Liquid Semiconductors, ed (J. Tauc, Plenum) 159 (1974).
- [18] C. Frigeri, L. Nasi, M. Serenyi, A. Csik, Z. Erdelyi, D. L. Beke, Superlatt. Microstruct 45,475 (2009).
- [19] A. A. Langford, M. L. Fleet, B. P. Nelson, W. A. Lanford and N. Maley, Phys. Rev. B 45, 13367 (1992).
- [20] J. A. Augis, J. E. Bennett, J. Thermal Anal. 13, 283 (1978).



الفهرس

الصفحة	اسم الباحث	عنوان البحث	ر.ت
1-23	يونس يوسف أبونايجي	وضع الضاهر موضع الضمير ودلالته على المعنى عند المفسرين	1
24-51	محمد خليفة صالح خليفة محمود الجداوي	دراسة استقصائية حول مساهمة تقنية المعلومات والاتصالات في نشر ثقافة الشفافية ومحاربة الفساد	2
52-70	Ebtisam Ali Haribash	An Interactive GUESS Method for Solving Nonlinear Constrained Multi-Objective Optimization Problem	3
71-105	احمد علي الهادي الحويج احمد محمد سليم معوال	العوامل الخمسة الكبرى للشخصية وعلاقتها بالذكاء الوجداني لدى طلبة مرحلة التعليم الثانوي	4
106-135	محمد عبد السلام دخيل	في المجتمع الليبي التحضر وانعكاساته على الحياة الاجتماعية "دراسة ميدانية في مدينة الخمس"	5
136-158	سالم فرج زويبيك	الاستعارة التهكمية في القرآن الكريم	6
159-173	أسماء جمعة القلعي	دور الرياضات العملية الصوفية في تهذيب السلوك	7
174-183	S. M. Amsheri N. A. Abouthferah	On Coefficient Bounds for Certain Classes of Analytic Functions	8
184-191	N. S. Abdanabi	Fibrewise Separation axioms in Fibrewise Topological Group	9
192-211	Samah Taleb Mohammed	Investigating Writing Errors Made by Third Year Students at the Faculty of Education El-Mergib University	10
212-221	Omar Ali Aleyan Eissa Husen Muftah AL remali	SOLVE NONLINEAR HEAT EQUATION BY ADOMIAN DECOMPOSITION METHOD [ADM]	11
222-233	حسن احمد قرقد عبدالباسط محمد قريصة مصطفى الطويل	قياس تركيز بعض العناصر الثقيلة في المياه الجوفية لمدينة مصراته	12
234-244	ربيعة عبد الله الشبير عائشة أحمد عامر عبير مصطفى الهصيك	تعادم الدوال الكروية المناظرة لقيم ذاتية على سطح الكرة	13
245-255	Khadiga Ali Arwini Entisar Othman Laghah	λ -Generalizations And g - Generalizations	14



256-284	خيري عبدالسلام حسين كليب عبدالسلام بشير اشتيوي بشير ناصر مختار كصارة	Impact of Information Technology on Supply Chain management	15
285-294	Salem H. Almadhun, Salem M. Aldeep, Aimen M. Rmis, Khairia Abdulsalam Amer	Examination of 4G (LTE) Wireless Network	16
295-317	نور الدين سالم فريوع	التجربة الجمالية لدى موريس ميرلوبوتي	17
318-326	ليلى منصور عطية الغويج هدى على التقبي	Effect cinnamon plant on liver of rats treated with trichloroethylene	18
327-338	Fuzi Mohamed Fartas Naser Ramdan Amaizah Ramdan Ali Aldomani Husamaldin Abdualmawla Gahit	Qualitative Analysis of Aliphatic Organic Compounds in Atmospheric Particulates and their Possible Sources using Gas Chromatography Mass Spectrometry	19
339-346	E. G. Sabra A. H. EL- Rifae	Parametric Tension on the Differential Equation	20
347-353	Amna Mohamed Abdelgader Ahmed	Totally Semi-open Functions in Topological Spaces	21
354-376	زينب إمام أبو راس حواء بشير بالنور	كتاب الخصائص لابن جني دراسة بعض مواضع الحذف من ت"392" المسمى: باب في شجاعة العربية	22
377-386	لطيفة محمد الدالي	Least-Squares Line	23
387-397	نادية محمد الدالي ايمان احمد اخميرة	THEORETICAL RESEARCH ON AI TECHNOLOGIES FOR LEARNING SYSEM	24
398-409	Ibrahim A. Saleh Tarek M. Fayez Mustafah M. A. Ahmad	Influence of annealing and Hydrogen content on structural and optoelectronic properties of Nano-multilayers of a-Si:H/a-Ge: H used in Solar Cells	25
410-421	أسماء محمد الحبشي	The learners' preferences of oral corrective feedback techniques	26
422-459	أمينة محمد العكاشي ربيعة عثمان عبد الجليل عفاف محمد بالحاج فتحية علي جعفر	التقدير الإيجابي المسبق لفاعلية الذات ودوره في التغلب على مصادر الضغوط النفسية " دراسة تحليلية "	27



460-481	Aisha Mohammed Ageal Najat Mohammed Jaber	English Pronunciation problems Encountered by Libyan University Students at Faculty of Education, Elmergib University	28
482-499	الحسين سليم محسن	The Morphological Analysis of the Quranic Texts	29
500-507	Ghada Al-Hussayn Mohsen	Cultural Content in Foreign Language Learning and Teaching	30
508-523	HASSAN M. ALI Mostafa M Ali	The relationship between <i>slyA</i> DNA binding transcriptional activator gene and <i>Escherichia coli</i> fimbriae and related with biofilm formation	31
524-533	Musbah A. M. F. Abduljalil	Molecular fossil characteristics of crude oils from Libyan oilfields in the Zalla Trough	32
534-542	سعدون شهبوب محمد	تلوث المياه الجوفية بالنترات بمنطقة كعام، شمال غرب ليبيا	33
543-552	Naima M. Alsharif Mahmoud M. Buazzi	Analysis of Genetic Diversity of <i>Escherichia Coli</i> Isolates Using RAPD PCR Technique	34
553-560	Hisham mohammed alnaib alshareef aisha mohammed elfagaeh aisha omran alghawash abdualaziz ibrahim lawej safa albashir hussain kaka	The Emergence of Virtual Learning in Libya during Coronavirus Pandemic	35
561-574	Abdualaziz Ibrahim Lawej Rabea Mansur Milad Mohamed Abduljalil Aghnayah Hamza Aabeed Khalafllaa ³	ATTITUDES OF TEACHERS AND STUDENTS TOWARDS USING MOTHER TONGUE IN EFL CLASSROOMS IN SIRTE	36
575-592	صالحة التومي الدروقي أمال محمد سالم أبوسته	دافع الانجاز وعلاقته بالرضا الوظيفي لدى معلمي مرحلة التعليم الأساسي "ببلدية ترهونة"	37
593-609	آمنة سالم عبد القادر قدورة نجية علي جبريل انبية	الإرشاد النفسي ودوره في مواجهة بعض المشكلات الأخرية الراهنة	38
610-629	Hanan B. Abousittash, Z. M. H. Kheiralla Betiha M.A.	Effect Mesoporous silica silver nanoparticles on antibacterial agent Gram- negative <i>Pseudomonas aeruginosa</i> and Gram-positive <i>Staphylococcus aureus</i>	39
630-652	حنان عمر بشير الرمالي	برنامج التربية العملية وتطويره	40
653-672	Abdualla Mohamed Dhaw	Towards Teaching CAT tools in Libyan Universities	41



673-700	عثمان علي أميمن سليمة رمضان الكوت زهرة عثمان البرق	سبل إعادة أعمار وتأهيل سكان المدن المدمرة بالحرب ومعوقات المصالحة الوطنية في المجتمع الليبي: مقارنة نفس-اجتماعية	42
701-711	Abdulrhman Mohamed Egnebr	Comparison of Different Indicators for Groundwater Contamination by Seawater Intrusion on the Khoms city, Libya	43
712-734	Elhadi A. A. Maree Abdualah Ibrahim Sultan Khaled A. Alurffi	Hilbert Space and Applications	44
735-759	معتوق علي عون عمار محمد الزليطني عرفات المهدي قرينات	الموارد الطبيعية اللازمة لتحقيق التنمية الاقتصادية بشمال غرب ليبيا وسبل تحقيق الاستدامة	45
760-787	سهام رجب العطوي هدى المبروك موسى	الخلج وعلاقته بمفهوم الذات لدى تلاميذ الشق الثاني بمرحلة التعليم الاساسي بمنطقة جنزور	46
788-820	هنية عبدالسلام بالوص زهرة المهدي أبو راس	الصلابة النفسية ودورها الوقائي في مواجهة الضغوط النفسية	47
821-847	عبد الحميد مفتاح أبو النور محي الدين علي المبروك	ودوره في الحد من التمر التوجيه التربوي والإرشاد النفسي المدرسي	48
848	الفهرس		52